Hindawi
Mathematical Problems in Engineering
Volume 2020, Article ID 7929157, 8 pages
https://doi.org/10.1155/2020/7929157

Research Article

Analysis of the Mechanical Characteristics of Bolts under Roof Separation Based on Exponential Function

Xiao Ding[1] **and Shuan-Cheng Gu**[2]

[1]*School of Civil & Architecture Engineering, Xi'an Technological University, No. 2 Xuefu Rd (M), Xi'an 710021, China*
[2]*School of Architecture and Civil Engineering, Xi'an University of Science and Technology, No. 58 Yanta Rd (N) Mid-Section, Xi'an 710054, China*

Correspondence should be addressed to Xiao Ding; dx_0402@163.com

Received 29 May 2020; Accepted 9 July 2020; Published 3 August 2020

Academic Editor: David Bassir

With regard to the excavation of coal mine tunnels, the phenomenon of roof separation frequently occurs owing to the deformation of roadway surrounding rocks, and the analysis of the influence of surrounding rock separation on bolt reinforcement plays an indispensable role in the security of support engineering. In the present paper, the hyperbolic function model of bolt load transfer is simplified to the exponential function form, and the simplified distribution form is modified by error analysis. Drawing on the analytic model of elastoplastic mechanics of bolt load through separation, this paper further investigates the influence of separation development on bolt load and conducts the parametric analysis of the separation value and separation position. Finally, taking the separation effect into consideration in the anchorage design of coal mine, practical reference value has been attached to the supporting design of underground engineering in bedded rock mass.

1. Introduction

Owing to the significant advantages, bolting support has been widely applied in the reinforcement of rock mass in mine engineering and the underground excavation support [1–3]. In recent years, many researchers have conducted studies concerning the mechanical characteristics and achieved fruitful results. Farmer [4] explored the mechanical characteristics of the bolt under pull-out load. It was considered that the axial force and interface shear stress of the bolt decay exponentially along the length direction with a small load. Freeman [5] proposed the neutral point theory of the stress status of bolts and reasonably explained the mechanical characteristics of bolts as a result of the deformation of surrounding rocks. Considering the property of shear modulus of adhesive layer with depth, Kumar and Khan [6] adopted the shear-lag theory to analyze the mechanical characteristics of bonded bolt. Based on the trilinear bond-slip model and transfer matrix method, Zheng and Dai [7] made a thorough analysis of the mechanical characteristics of grouted FRP rods in steel tubes in the drawing process. Cai et al. [8] employed the shear model of two-stage linear function to describe the mechanical process of bolt anchorage interface under external force and analyze the coupling and decoupling mechanism of bolt force with the deformation of surrounding rocks in the circular tunnel.

Coal mine roadways supported by bolts are mostly composed of layered sedimentary rocks. The incompatible deformation of rocks will lead to the roof separation, whose expansion generates the addition drawing load. The excessive separation will make the bolt invalid and results in potential safety hazards. Li and Stillborg [9] and Cai et al. [10] carried out a systematic study on the bolt load in fractured rock mass and proposed the mechanical distribution form of bolt in jointed rock mass. Windsor and Thompson [11] gave a qualitative description of the stress of bolts with the occurrence of cracks in surrounding rocks. Li [12] pointed out that the occurrence of cracks in anchored rock mass would exercise tension on the bolt, and a static load test was designed to measure the stress distribution

subjected to the opening of rock joints, followed by the impact test [13]. With regard to the failure modes of bolts in jointed rock mass, Nie et al. [14] made an elaborate summary and implemented the joint bolt element in DDA program. Based on the literature above, studies have not been comprehensively conducted in terms of the establishment of mechanical analysis model of bolt under rock mass separation (joints) and the existing models fail to consider the effect of separation position on the load acting on bolts.

This paper, according to the mechanism of pull-out load acting on bolt, puts forward a mechanical model of additional stress of bolt anchorage as a result of separation. The mechanical distribution of hyperbolic function is simplified and revised, and the mechanical distribution of bolt anchorage in elastic and elastic-plastic state under the action of separation is obtained therefrom. Moreover, an in-depth analysis is conducted of the parameters of the value and position of separation. Considering the influence of separation on bolt, a new design idea of roadway support is put forward in this paper.

2. Load Analysis under the Action of Separation

2.1. Stress Distribution of Bolt Anchorage under Elastic State. In the previous study conducted by Ding et al. [15, 16], the hyperbolic function distribution form of axial force and interfacial shear stress of bolt anchorage subjected to separation in the elastic state is deduced based on the establishment of static equilibrium equation for anchor microsegment.

Left side (from the roadway surface to the separation) is

$$\tau_1(x) = \frac{\beta P_0 \mathrm{ch}(\beta x)}{\pi D \mathrm{sh}(\beta x_0)}, \tag{1}$$

$$P_1(x) = \frac{P_0 \mathrm{sh}(\beta x)}{\mathrm{sh}(\beta x_0)}. \tag{2}$$

Right side (from the separation to the end of bolt) is

$$\tau_2(x) = \frac{\beta P_0 \mathrm{ch}[\beta(L-x)]}{\pi D \mathrm{sh}[\beta(L-x_0)]}, \tag{3}$$

$$P_2(x) = \frac{P_0 \mathrm{sh}[\beta(L-x)]}{\mathrm{sh}[\beta(L-x_0)]}, \tag{4}$$

where L is the bolt length; x is the distance from roadway surface; x_0 is the position of separation (also the distance from separation to roadway surface); P_0 is the axial tensile force generated by separation on both sides of bolt anchorage; β is the coefficient related to bolt and surrounding rock, $\beta = \sqrt{4K/(\pi D^2 E_a)}$; K is the shear stiffness coefficient, which is related to surrounding rock and grouting material; D is the diameter of the borehole; d is the diameter of the bolt; and $E_a = (E_g(D^2 - d^2) + E_b d^2)/D^2$ is the composite elastic modulus, where E_b is the elastic modulus of bolts and E_g is the elastic modulus of grout.

2.2. Simplification of Hyperbolic Function. It can be found that $L \gg 1/\beta$ under normal conditions based on the parametric analysis of hyperbolic function in terms of shear stress and axial force of bolt anchorage. When $e^{\beta L} \gg e^{-\beta L}$ with the difference of three orders of magnitude, also $\beta L \geq 2.31$, then $e^{-\beta L}$ can be omitted (which is also true of $e^{-\beta x}$). Formulae (1)–(4) can be reduced to exponential function.

Simplification of left side is

$$\tau_{1_J}(x) = \frac{\beta P_0}{\pi D} e^{\beta(x-x_0)}, \tag{5}$$

$$P_{1_J}(x) = P_0 e^{\beta(x-x_0)}. \tag{6}$$

Simplification of right side is

$$\tau_{2_J}(x) = \frac{\beta P_0}{\pi D} e^{-\beta(x-x_0)}, \tag{7}$$

$$P_{2_J}(x) = P_0 e^{-\beta(x-x_0)}. \tag{8}$$

By comparison of the stress distributions of the two different functions, errors will occur, especially larger at the boundary, with a short length of bolts. Owing to the uncertain position of separation, the length of bolts on both sides presents differences. In this regard, the simplified exponential form should be revised to avoid large errors due to the shorter length. The revised shear stress and axial force at the interface of bolt anchorage are presented as follows.

Based on the simplification and revision for the left side, the simplified form is assumed as $P'_{1_J}(x) = A_1 P_0 e^{\beta(x-x_0)} + B_1$. According to the boundary condition, $P'_{1_J}|_{x=0} = 0$ and $P'_{1_J}|_{x=x_0} = P_0$, we can obtain $A_1 = 1/(1 - e^{-\beta x_0})$ and $B_1 = P_0/(1 - e^{\beta x_0})$:

$$P'_{1_J}(x) = \frac{P_0}{e^{\beta x_0} - 1}\left(e^{\beta x} - 1\right). \tag{9}$$

Then, the following expression can be obtained according to the relationship between axial force and shear stress:

$$\tau'_{1_J}(x) = \frac{\beta P_0}{\pi D\left(e^{\beta x_0} - 1\right)} e^{\beta x}. \tag{10}$$

Similarly, the right side is simplified and adjusted:

$$P'_{2_J}(x) = \frac{P_0}{e^{\beta(L-x_0)} - 1}\left[e^{\beta(L-x)} - 1\right], \tag{11}$$

$$\tau'_{2_J}(x) = \frac{\beta P_0}{\pi D\left[e^{\beta(L-x_0)} - 1\right]} e^{\beta(L-x)}. \tag{12}$$

Drawing on the parameters in Section 3.2, the axial force, as well as the shear stress at the surface of bolt anchorage using three function models, is analyzed by taking the separation occurring at 0.6 m away from the roadway wall and the separation value $b = 0.04$ mm as an example, as shown in Figures 1 and 2.

As Figures 1 and 2 indicate, the modified exponential form of the axial force of bolt anchorage is basically consistent with the hyperbolic function distribution. The

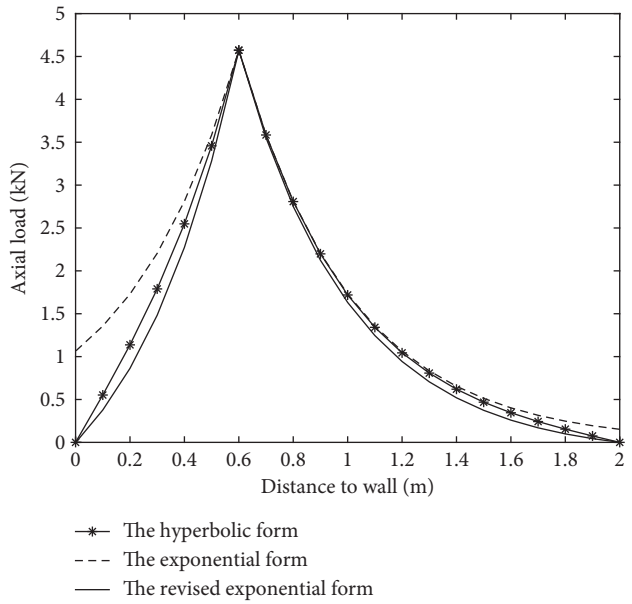

Figure 1: The axial force distribution of bolt anchorage with different forms of function.

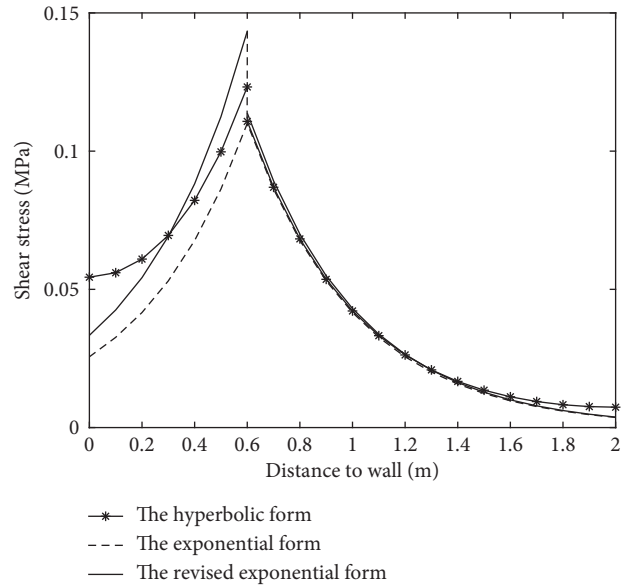

Figure 2: The sheer stress distribution of bolt anchorage with different forms of function.

modified exponential form is used to calculate the shear stress at the interface of the bolt anchorage. The value at the separation is slightly larger than that of the hyperbolic function, and the value at both ends is smaller than that of the hyperbolic function. In this paper, the revised exponential function is adopted, which is easier to calculate than hyperbolic function.

At the elastic state, the separation value b can be regarded as the sum of the elongation of bolt anchorage on the left and right sides. In view of this condition, the relationship between the separation value b and the axial tension P_0 at the separation can be deduced:

$$P_0 = \frac{\pi D^2 \beta E_a b}{4\omega}, \tag{13}$$

where $\omega = [2 - (\beta x_0/(e^{\beta x_0} - 1)) - (\beta(L - x_0)/(e^{\beta(L-x_0)} - 1))]$. Put the above equation into formulae (9)–(12).

Left side is

$$\tau'_{1_J}(x) = \frac{\beta^2 E_a D e^{\beta x}}{4\omega(e^{\beta x_0} - 1)} b, \tag{14}$$

$$P'_{1_J}(x) = \frac{\pi D^2 \beta E_a (e^{\beta x} - 1)}{4\omega(e^{\beta x_0} - 1)} b. \tag{15}$$

Right side is

$$\tau'_{2_J}(x) = \frac{\beta^2 E_a D e^{\beta(L-x)}}{4\omega\left[e^{\beta(L-x_0)} - 1\right]} b, \tag{16}$$

$$P'_{2_J}(x) = \frac{\pi D^2 \beta E_a \left[e^{\beta(L-x)} - 1\right]}{4\omega\left[e^{\beta(L-x_0)} - 1\right]} b. \tag{17}$$

As formulae (14)–(17) show, the interfacial shear stress and axial force of bolt anchorage in the elastic state are linearly related to the separation value b but nonlinearly related to the position of separation x_0.

3. Establishment and Analysis of the Elastoplastic Model

3.1. Establishment of the Elastoplastic Model. When the shear stress on the interface between bolts anchorage and surrounding rocks exceeds the shear strength of the interface, the debonding and destruction of the interface will occur, signifying the entering into the elastic-plastic stage. At the same time, the deformation of the bolt anchorage on both sides of the separation can be divided into plastic deformation and elastic deformation.

In this present paper, the shear slip model of the two-stage linear function is adopted to calculate the slip range L_{s1} and L_{s2} on both left and right sides [17].

Left side is

$$L_{s1} = \frac{P_0}{\pi D \tau_s}\left[1 - \frac{e^{\beta(x_0 - L_{01})} - 1}{e^{\beta x_0} - 1}\right]. \tag{18}$$

Right side is

$$L_{s2} = \frac{P_0}{\pi D \tau_s}\left[1 - \frac{e^{\beta(L - x_0 - L_{02})} - 1}{e^{\beta(L-x_0)} - 1}\right], \tag{19}$$

where $L_{01} = x_0 - (1/\beta)\ln[(\pi D \tau_e/\beta P_0)(e^{\beta x_0} - 1)]$; $L_{02} = L - x_0 - (1/\beta)\ln[(\pi D \tau_e/\beta P_0)[e^{\beta(L-x_0)} - 1]]$; τ_e is bond strength of initial anchor between bolts and rocks; and τ_s is the bond strength of L_s in the slip range after entering the plastic stage.

In this regard, the distribution of shear stress and axial force of the bolt anchorage is obtained under the elastic-plastic state, as shown in Figure 3.

Plasticity on the left side is

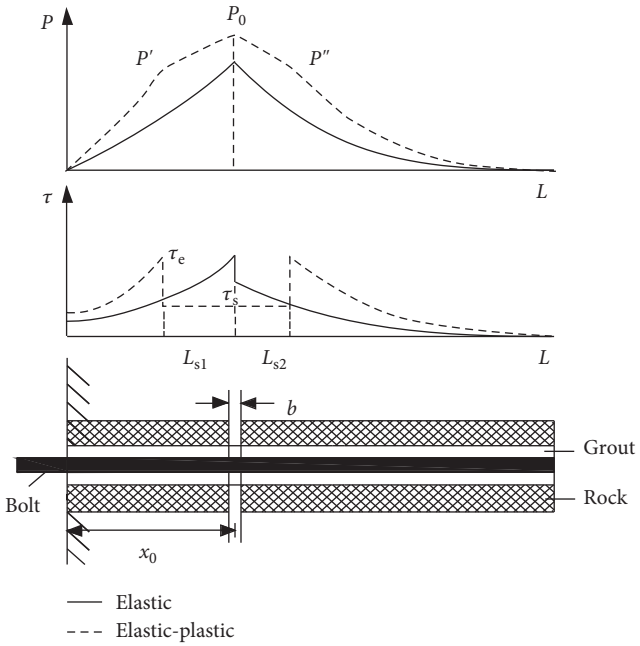

Figure 3: Distribution of shear stress and axial force of bolt anchorage with single separation under the elastic-plastic state.

$$\tau_1^p(x) = \tau_s, \tag{20}$$

$$P_1^p(x) = P_0 + \pi D\tau_s(x - x_0). \tag{21}$$

Plasticity on the right side is

$$\tau_2^p(x) = \tau_s, \tag{22}$$

$$P_2^p(x) = P_0 - \pi D\tau_s(x - x_0). \tag{23}$$

Elasticity on the left side is

$$\tau_1^e(x) = \frac{\beta P_{e1} e^{\beta(x+L_{s1})}}{\pi D\left(e^{\beta x_0} - 1\right)}, \tag{24}$$

$$P_1^e(x) = \frac{P'\left(e^{\beta x} - 1\right)}{e^{\beta(x_0 - L_{s1})} - 1}. \tag{25}$$

Elasticity on the right side is

$$\tau_2^e(x) = \frac{\beta P_{e2} e^{\beta(L-x+L_{s2})}}{\pi D\left[e^{\beta(L-x_0)} - 1\right]}, \tag{26}$$

$$P_2^e(x) = \frac{P''\left[e^{\beta(L-x)} - 1\right]}{e^{\beta(L-x_0-L_{s2})} - 1}. \tag{27}$$

where $P' = P_0 - \pi D\tau_s L_{s1}$ and $P'' = P_0 - \pi D\tau_s L_{s2}$.

Suppose that P_{e1} and P_{e2} are the ultimate drawing force of bolts in the critical sliding state on both left and right sides. According to formulae (1) and (3), we can obtain

$$P_{e1} = \frac{\pi D\tau_e}{\beta}\left(1 - e^{-\beta x_0}\right), \tag{28}$$

$$P_{e2} = \frac{\pi D\tau_e}{\beta}\left[1 - e^{-\beta(L-x_0)}\right]. \tag{29}$$

Considering the interfacial debonding, the expression of separation value b is presented as follows:

(1) x_0 is located on the left side of bolts, close to the wall of roadway. When $P_{e1} < P_0 < P_{e2}$, the interface of the left bolt anchorage begins to slip and enters the elastic-plastic stage, while the right side is still in the elastic stage:

$$\begin{aligned} b_1 = \xi_1 + \xi_2 &= \int_0^{x_0} \varepsilon_1 \mathrm{d}x + \int_{x_0}^{L} \varepsilon_2 \mathrm{d}x = \frac{4}{\pi D^2 E_a}\int_0^{x_0} P_1(x)\mathrm{d}x \\ &\quad + \frac{4}{\pi D^2 E_a}\int_{x_0}^{L} P_2(x)\mathrm{d}x \\ &= \frac{4}{\pi D^2 E_a}\left[\int_0^{x_0-L_{s1}} \frac{P'\left(e^{\beta x} - 1\right)}{e^{\beta(x_0-L_{s1})} - 1}\mathrm{d}x \right. \\ &\quad + \int_{x_0-L_{s1}}^{x_0} \left[P_0 + \pi D\tau_s(x - x_0)\right]\mathrm{d}x \\ &\quad \left. + \int_{x_0}^{L} \frac{P_0\left[e^{\beta(L-x)} - 1\right]}{e^{\beta(L-x_0)} - 1}\mathrm{d}x\right]. \end{aligned} \tag{30}$$

If $P_0 > P_{e2}$, the interface on left and right sides of the separation enters the elastic-plastic stage:

$$\begin{aligned} b_2 = \xi_1 + \xi_2 &= \int_0^{x_0} \varepsilon_1 \mathrm{d}x + \int_{x_0}^{L} \varepsilon_2 \mathrm{d}x = \frac{4}{\pi D^2 E_a}\int_0^{x_0} P_1(x)\mathrm{d}x \\ &\quad + \frac{4}{\pi D^2 E_a}\int_{x_0}^{L} P_2(x)\mathrm{d}x \\ &= \frac{4}{\pi D^2 E_a}\left[\int_0^{x_0-L_{s1}} \frac{P'\left(e^{\beta x} - 1\right)}{e^{\beta(x_0-L_{s1})} - 1}\mathrm{d}x \right. \\ &\quad + \int_{x_0-L_{s1}}^{x_0} \left[P_0 + \pi D\tau_s(x - x_0)\right]\mathrm{d}x \\ &\quad + \int_{x_0}^{x_0+L_{s2}} \left[P_0 - \pi D\tau_s(x - x_0)\right]\mathrm{d}x \\ &\quad \left. + \int_{x_0+L_{s2}}^{L} \frac{P''\left[e^{\beta(L-x)} - 1\right]}{e^{\beta(L-x_0-L_{s2})} - 1}\mathrm{d}x\right]. \end{aligned} \tag{31}$$

As the above equation shows, $x_0 \neq L_{s1}$. When the left side enters the plastic stage, $x_0 = L_{s1}$, the separation value is

$$\begin{aligned} b_3 = \xi_1 + \xi_2 &= \int_0^{x_0} \varepsilon_1 \mathrm{d}x + \int_{x_0}^{L} \varepsilon_2 \mathrm{d}x = \frac{4}{\pi D^2 E_a} \\ &\quad \times \int_0^{x_0} P_1(x)\mathrm{d}x + \frac{4}{\pi D^2 E_a} \int_{x_0}^{L} P_2(x)\mathrm{d}x \\ &= \frac{4}{\pi D^2 E_a} \left[\int_0^{x_0} \left[P_0 + \pi D \tau_s (x - x_0) \right] \mathrm{d}x \right. \\ &\quad + \int_{x_0}^{x_0 + L_{s2}} \left[P_0 - \pi D \tau_s (x - x_0) \right] \mathrm{d}x \\ &\quad \left. + \int_{x_0 + L_{s2}}^{L} \frac{P'' \left[e^{\beta (L - x)} - 1 \right]}{e^{\beta (L - x_0 - L_{s2})} - 1} \mathrm{d}x \right]. \end{aligned} \tag{32}$$

(2) x_0 is located on the right side of bolts, close to the interior of rock mass. When $P_{e2} < P_0 < P_{e1}$, the interface of the right bolt anchorage begins to slip and enters the elastic-plastic stage, while the left side is still in the elastic stage:

$$\begin{aligned} b_1' = \xi_1 + \xi_2 &= \int_0^{x_0} \varepsilon_1 \mathrm{d}x + \int_{x_0}^{L} \varepsilon_2 \mathrm{d}x = \frac{4}{\pi D^2 E_a} \int_0^{x_0} P_1(x)\mathrm{d}x \\ &\quad + \frac{4}{\pi D^2 E_a} \int_{x_0}^{L} P_2(x)\mathrm{d}x \\ &= \frac{4}{\pi D^2 E_a} \left[\int_0^{x_0} \frac{P_0 \left(e^{\beta x} - 1 \right)}{e^{\beta x_0} - 1} \mathrm{d}x \right. \\ &\quad + \int_{x_0}^{x_0 + L_{s2}} \left[P_0 - \pi D \tau_s (x - x_0) \right] \mathrm{d}x \\ &\quad \left. + \int_{x_0 + L_{s2}}^{L} \frac{P'' \left[e^{\beta (L - x)} - 1 \right]}{e^{\beta (L - x_0 - L_{s2})} - 1} \mathrm{d}x \right]. \end{aligned} \tag{33}$$

If $P_0 > P_{e1}$, the interface on the left and right sides of the separation enters the elastic-plastic stage, $b_2' = b_2$ (L-$x_0 \neq L_{s2}$). When the right side of bolts all enters the plastic stage, that is, L-$x_0 = L_{s2}$, and the separation value is

$$\begin{aligned} b_3' = \xi_1 + \xi_2 &= \int_0^{x_0} \varepsilon_1 \mathrm{d}x + \int_{x_0}^{L} \varepsilon_2 \mathrm{d}x = \frac{4}{\pi D^2 E_a} \int_0^{x_0} P_1(x)\mathrm{d}x \\ &\quad + \frac{4}{\pi D^2 E_a} \int_{x_0}^{L} P_2(x)\mathrm{d}x \\ &= \frac{4}{\pi D^2 E_a} \left[\int_0^{x_0 - L_{s1}} \frac{P' \left(e^{\beta x} - 1 \right)}{e^{\beta (x_0 - L_{s1})} - 1} \mathrm{d}x \right. \\ &\quad + \int_{x_0 - L_{s1}}^{x_0} \left[P_0 + \pi D \tau_s (x - x_0) \right] \mathrm{d}x \\ &\quad \left. + \int_{x_0}^{L} \left[P_0 - \pi D \tau_s (x - x_0) \right] \mathrm{d}x \right]. \end{aligned} \tag{34}$$

Formulae (30)–(34) present the relationship between separation value b and the axial tensile force P_0 under elastic-plastic conditions. According to the value b of separation, the corresponding P_0 can be obtained, and by substituting P_0 into formulae (18) and (19), the slip ranges of L_{s1} and L_{s2} on both sides are determined. Moreover, based on formulae (14)–(17), (20)–(27) give the distribution of shear stress and axial force at the interface of bolt anchorage with the elastic and elastic-plastic states.

3.2. Stress Distribution of Bolt Anchorage under Elastic-Plastic State. Based on the research on bolt support project of transportation roadway in N1203 fully Mechanized Mining Face of Ning tiao-ta Coal Mine in Northern Shaanxi, the length of the bolt is 2 m, the diameter of the borehole is 32 mm, the diameter of the bolt is 20 mm, and the rock mass around the bolt is sandstone, which is relatively complete. Furthermore, the elastic modulus is 2 GPa, Poisson's ratio is $\mu = 0.23$, the cohesion is $c = 1.12$ MPa, the internal friction angle is $\phi = 38°$, and the shear stiffness coefficient is $K = 0.4$ GPa/m. Besides, the elastic modulus of bolt is 200 GPa, the elastic modulus of grout is 10 GPa, the initial bond strength between anchor and rock is 0.6 MPa, and the bond strength after entering the plastic stage is 0.4 MPa. By the aid of borehole sight instrument, it has been found that the separation appears in the surrounding rocks of roadway in the field test, which is 0.5 m away from the wall. The stress distribution of bolt anchorage is calculated and analyzed in the following. Figure 4 presents the distribution curves of shear stress and axial force of bolt anchorage with the separation value b of 0.1 mm, 0.2 mm, 0.28 mm, and 0.4 mm. Figure 5 shows the relationship between the separation value and the axial force at the separation.

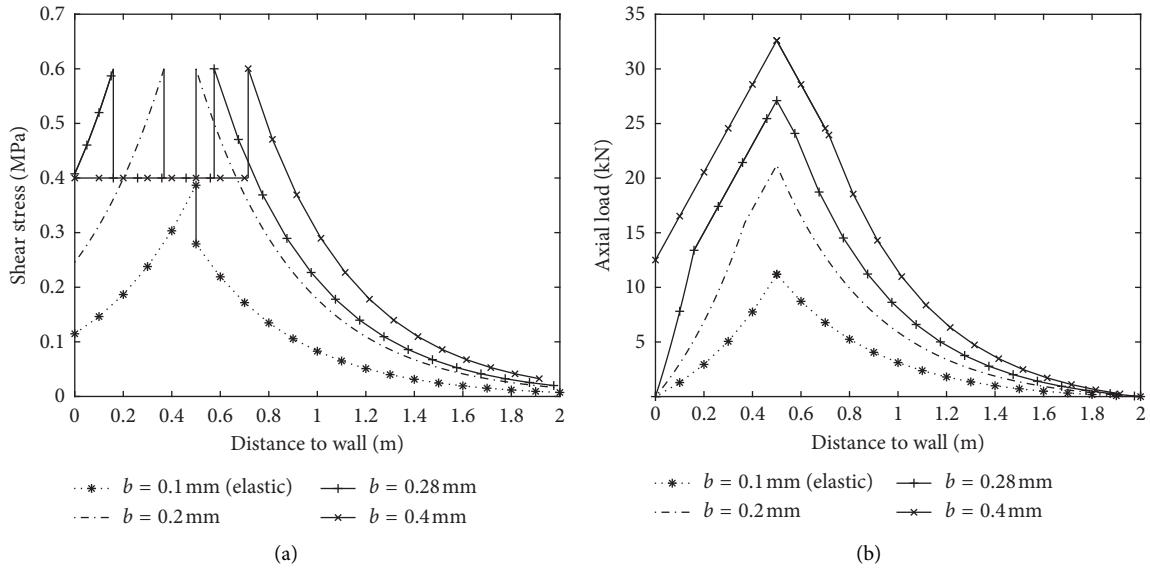

Figure 4: Distribution curves of shear stress and axial force of bolt anchorage at different separation levels with the same position. (a) The interfacial shear stress distribution curve of bolt anchorage with different separation values. (b) The axial force distribution curve of bolt anchorage with different separation values.

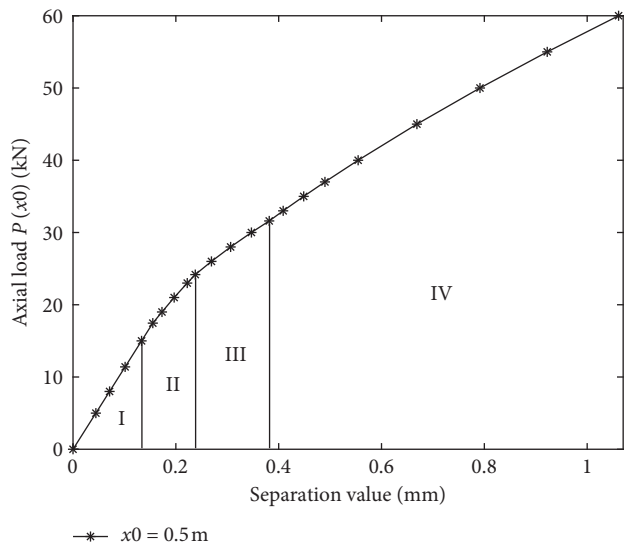

Figure 5: The relation curve between separation value and axial force of bolt anchorage.

As Figure 4 indicates, the separation occurs at 0.5 m. With the separation equal to 0.1 mm, the interface between the left and right sides is under the elastic state, and the axial force is equal to 11.2 kN at both sides. Owing to the sudden change, the shear stress of the left bolt anchorage is larger than that on the right with the maximum value of 0.39 MPa. As the value increases to 0.2 mm, the interface on the left bolt anchorage enters the plastic stage, 0.132 m away from the separation position, in which the shear stress is 0.4 MPa, with the maximum value of 0.6 MPa on the right, and the maximum axial force is 21.2 kN. When reaching 0.28 mm, the left anchorage interface of separation enters the plastic stage, 0.341 m near the separation, and the right interface is under the plastic stage of 0.075 m, with the maximum axial force of 27.1 kN. As the value increases to 0.4 mm, the left anchorage interface of separation all enters the plastic stage, while the right is at the plastic stage, 0.215 m away from the separation, with the maximum axial force of 32.6 kN. In this regard, conclusions can be drawn that the larger the separation value, the greater the axial force of bolt anchorage and the interfacial shear stress.

As Figure 5 indicates, with the increase of separation value, the axial force of bolt anchorage at the separation also presents an increasing trend. The whole variation process is composed of four stages (I–IV). Stage I refers to the elastic stage, where there exists a linear relation between the separation value and the axial force of bolt anchorage. Stage II is the elastoplastic stage from the left side with the right side still being in the elastic stage. Stage III signifies the entering of elastoplastic stage from the right side with an increasing slip range of the left side. Stage IV marks all the left side entrances in the plastic stage with an increasing slip range of the right side.

4. Roadway Support Design

A flow chart of roadway support design considering separation effect is shown in Figure 6.

The support design is adopted for N1203 fully Mechanized Mining Face of Liantaota Coal Mine in Northern Shaanxi. According to the support parameters in Section 3.2, it can be calculated from [18, 19] that in the case of no separation, the maximum load of the bolt is 20.4 kN, which is less than the ultimate bearing capacity of 54 kN, signifying the security of support. By aid of the roof separation monitoring system, detection is given that the separation occurs at 0.9 m away from the roadway wall with the value of 5 mm. The theoretical calculation shows that the maximum

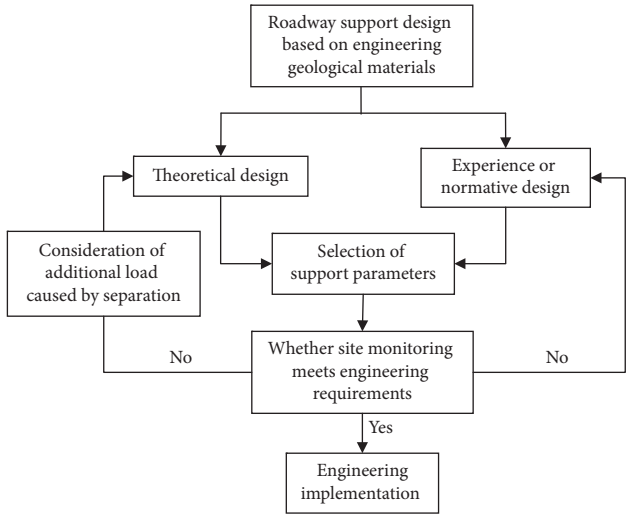

Figure 6: The flow chart of roadway support design.

load of the bolt increases 57 kN, which exceeds the ultimate bearing capacity of the bolt, losing the supporting function with great potential risks.

In this paper, the parameters of roadway support are adjusted considering the effect of separation, among which the length and diameter of bolts are changed to 2.5 m and 22 m, and the ultimate bearing capacity increases to 70 kN. In the case of no separation, the maximum load of bolts is 30.5 kN. However, with the roof separation, the maximum load of the bolt increases to 66 kN, which is less than the ultimate bearing capacity. Field construction monitoring shows that the support design method is much safe and more reliable.

5. Conclusions

(1) Additional stress of bolt will be produced by the roof separation of roadway. In this paper, the hyperbolic function model of load transfer of bolt is simplified, and the error analysis is conducted for modifying the simplified distribution form. Then the modified exponential function is used to establish an elastic-plastic mechanical analysis model for the bolt anchorage load generated by the separation.

(2) The influencing process of separation on the load of bolt anchorage consists of 4 stages, which are elastic stage, unilateral elastic-plastic stage, elastic-plastic stage of both sides of separation, and the stage of slipping on one side and increasing range of the other side. Based on the parametric analysis, the larger the separation value, the greater the load of bolt anchorage as a result of separation.

(3) Drawing on the analysis of the case study, the effect of separation on the load of bolts cannot be neglected. In the present paper, a new design idea of roadway support is put forward with the consideration of the bolt load generated by the separation in the original support design. Field construction monitoring shows that the support design method is much safer and more reliable.

Data Availability

The data used to support the findings of this study are included within the article.

Conflicts of Interest

The authors declare that they have no conflicts of interest regarding the publication of this paper.

Acknowledgments

The authors are grateful to the National Natural Science Foundation of China (No.11802218), the Science and Technology Planning Project of Shaanxi Province (2019JQ-432 and 2019JQ-835), and the Scientific Research Program funded by Shaanxi Provincial Education Department (No.19JK0399) for the financial support.

References

[1] C. R. Windsor, "Rock reinforcement systems," *International Journal of Rock Mechanics and Mining Sciences*, vol. 34, no. 6, pp. 919–951, 1997.

[2] X. Li, J. Nemcik, A. Mirzaghorbanali, N. Aziz, and H. Rasekh, "Analytical model of shear behaviour of a fully grouted cable bolt subjected to shearing," *International Journal of Rock Mechanics and Mining Sciences*, vol. 80, pp. 31–39, 2015.

[3] S. Ma, J. Nemcik, N. Aziz, and Z. Zhang, "Analytical model for rock bolts reaching free end slip," *Construction and Building Materials*, vol. 57, pp. 30–37, 2014.

[4] I. W. Farmer, "Stress distribution along a resin grouted rock anchor," *International Journal of Rock Mechanics and Mining Sciences & Geomechanics Abstracts*, vol. 12, no. 11, pp. 347–351, 1975.

[5] T. J. Freeman, "The behaviour of fully-bonded rock bolts in the Kielder experimental tunnel," *Tunnels & Tunnelling June*, vol. 10, no. 5, pp. 37–40, 1978.

[6] S. Kumar and M. A. Khan, "A shear-lag model for functionally graded adhesive anchors," *International Journal of Adhesion and Adhesives*, vol. 68, pp. 317–325, 2016.

[7] J.-J. Zheng and J.-G. Dai, "Analytical solution for the full-range pull-out behavior of FRP ground anchors," *Construction and Building Materials*, vol. 58, pp. 129–137, 2014.

[8] Y. Cai, T. Esaki, and Y. Jiang, "An analytical model to predict axial load in grouted rock bolt for soft rock tunnelling," *Tunnelling and Underground Space Technology*, vol. 19, no. 6, pp. 607–618, 2004.

[9] C. Li and B. Stillborg, "Analytical models for rock bolts," *International Journal of Rock Mechanics and Mining Sciences*, vol. 36, no. 8, pp. 1013–1029, 1999.

[10] Y. Cai, T. Esaki, and Y. Jiang, "A rock bolt and rock mass interaction model," *International Journal of Rock Mechanics and Mining Sciences*, vol. 41, no. 7, pp. 1055–1067, 2004.

[11] C. R. Windsor and A. G. Thompson, "Reinforcement systems mechanics, design, installation, testing, monitoring & modelling," *International Journal of Rock Mechanics and Mining Sciences*, vol. 35, no. 4-5, p. 453, 1998.

[12] C. C. Li, "Performance of D-bolts under static loading," *Rock Mechanics and Rock Engineering*, vol. 45, no. 2, pp. 183–192, 2012.

[13] C. C. Li and C. Doucet, "Performance of D-bolts under dynamic loading," *Rock Mechanics and Rock Engineering*, vol. 45, no. 2, pp. 193–204, 2012.

[14] W. Nie, Z. Y. Zhao, Y. J. Ning, and J. P. Sun, "Development of rock bolt elements in two-dimensional discontinuous deformation analysis," *Rock Mechanics and Rock Engineering*, vol. 47, no. 6, pp. 2157–2170, 2014.

[15] X. Ding, S. C. Gu, H. He, and Y. Zhang, "Force characteristic analysis of bolt under single and multiple bed separation," *Chinese Journal of Rock and Soil Mechanics*, vol. 40, no. 11, pp. 4299–4305, 2019.

[16] X. Ding, *Research on bolt load transfer mechanism under bed separation effect and its support designs*, Ph.D. thesis, Xi'an University of Science and Technology, Xi'an, China, 2016.

[17] J. Duan, Z. X. Yan, and R. J. Guo, "Failure analysis of soil anchors induced by loose interface under pullout load," *Chinese Journal of Geotechnical Engineering*, vol. 34, no. 5, pp. 936–941, 2012.

[18] R. A. Cook, G. T. Doerr, and R. E. Klingner, "Bond stress model for design of adhesive anchors," *ACI Structural Journal*, vol. 90, no. 5, pp. 514–524, 1993.

[19] M. S. Wang, "Mechanism of full-column rock bolt," *Chinese Journal of Coal Society*, vol. 8, no. 1, pp. 40–47, 1983.